LIQUID VAPOR ISOTHERMS IN NANO-POROUS MEDIA UNDER NMR OBSERVATION

Aleksandr Denisenko
Schlumberger Moscow Research Center

This paper was prepared for presentation at the International Symposium of the Society of Core Analysts held in Trondheim, Norway, 27-30 August 2018

ABSTRACT

Conventional experimental approaches and current understanding of low-permeability reservoir rocks are based on the models of hydrocarbon storage and transport in rather large pore systems (several microns and larger) where the properties of bounded fluids are close to the bulk ones and fluid flow in the rock complies with Darcy's law. This concept is not straightforward or useful for complex reservoirs with nanoscale pores. Instead, their characterization requires revisiting available petrophysical techniques. This work delivers a modern consideration of sorption processes of liquid vapor in porous media with a leading role given to nuclear magnetic resonance (NMR) phenomena. The high accuracy of the NMR method to hydrogen nuclei volume and especially its sensitivity to the surface properties of confining media enable discovering new potential adsorption-desorption mechanisms. This study presents the first step in experiments with artificial solid porous models and synthetic liquids, which could then be transposed to natural and more complex oil- and gas-bearing rocks.

INTRODUCTION

Core analysis practice has shown that obtaining accurate adsorption/desorption isotherms is highly important in studying confined fluids [1]. There are standard instruments for measuring them, but by including NMR it is possible to obtain much more information and to characterize in more detail the processes of fluid-rock interaction [2-3]. The use of NMR to measure adsorption isotherms is not entirely novel [4-6], but the use of T_1–T_2 correlation plots has not been applied to enhance the information potential of data acquired during a sorption process. Sorption processes studies combined with routine gas adsorption Brunauer-Emmett-Teller (BET) and NMR techniques could provide detailed information on sample pore geometry down to the nanometer scale as well as characterization of its surface properties. The latter is mostly governed by surface adhesion phenomena or wettability. It is widely observed in literature that wettability formulation of nanoscale porous objects is difficult and ambiguous [7], but complementary NMR study of adsorption/desorption processes shows encouraging evidence for developing an alternative wettability metric, which is based on the adsorption potential of the nanoscale pore [6].

This paper focuses on a successive study of artificial nanopore networks (called "mesoporous" in catalysis) saturated with pure synthetic fluids (i.e., water and liquid

alkanes), which is a necessary step before assessing the sophisticated properties of natural nanoporous rocks.

MEASUREMENT PROCEDURES AND APPARATUS

Liquid Vapor Sorption Technique Combined with NMR Registration

This technique uses a special liquid-filled tank connected to an NMR core-holder with a thermo-isolated tube. The temperature of the liquid in the tank is stabilized and can be manually set to generate the desired vapor pressure P above the liquid in the range of relative (partial) pressures P/P_0 between zero and unity, where P_0 is the pressure of the saturated liquid vapor at the temperature of the NMR magnet (~34°C). Therefore, adjusting the temperature in the tank modifies the partial vapor pressure in the NMR core-holder and the amount of sorbate correspondingly. The installation scheme is shown in Figure 1.

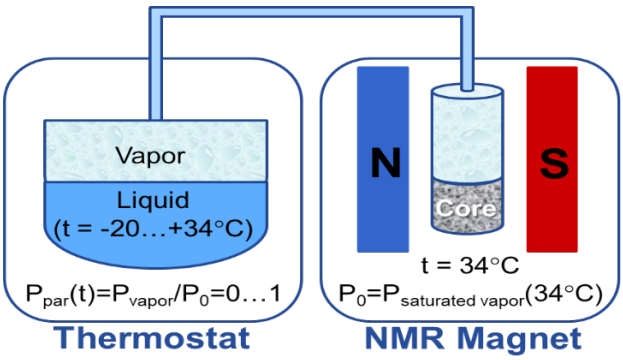

Figure 1. Experimental setup for studying adsorption/desorption processes in porous structures by NMR registration.

The experiments were conducted using two fluids: hexane and water. Depending on the liquid, the temperature of the thermostat ranged from –20°C to 34°C (hexane) or from –2°C to 34°C (water). Intermediate temperatures were selected to change the saturated vapor pressure in the core-holder on a relative scale from 0 to 1 in increments of 0.1.

Porous glass was used as an appropriate porous material to conduct the sorption experiments. This glass is manufactured from a borosilicate-based material that had been heated to separate the borates from the silica. The borates are leached out from the two-phase matrix, resulting in a silica glass with uniform and controlled pore sizes. Thus, porous glass is strongly water-wet pure-silica media. The following types of media were used as nanoporous sorbents:

- Controlled pore glass (CPG) from Asahi and Millipore with pore sizes of 50–300 nm;
- 4-nm and 10-nm porous glass manufactured by Advanced Glass and Ceramics.

Initial porometric measurements were processed using nitrogen sorption isotherms and the appropriate calculations based on the Barrett-Joyner-Halenda (BJH) method. The "nitrogen-sorption" pore sizes were additionally verified using high-field NMR-cryoporometry [8] and scanning electron microscopy (SEM) analyses.

For all samples, a complete cycle of the saturated vapor pressure variation was conducted. At each pressure point, the distributions of the relaxation times T_2 and T_1–T_2 were recorded. With an assumption of a liquid hydrogen index HI = 1, the NMR ^{1}H signal amplitude corresponds to the amount of adsorbed/desorbed fluid whereas the T_1 and T_2 data indicates both the confinement degree (pore geometry) and, most importantly, the ability of the solid phase to relax the hydrogen nucleus. The latter corresponds to many factors, including the wettability of pore surfaces.

NMR Equipment and Acquisition Procedures

All NMR measurements were conducted using an Oxford Instruments low-field spectrometer. The resonance frequency of 20.6 MHz corresponds to the hydrogen nuclei spin precession in a ~0.5T magnetic field. The relaxation decays of T_2 and T_1 were recorded by use of routine Carr-Purcell-Meiboom-Gill (CPMG) trains and inversion-recovery pulse sequence with the following parameters: echo time of 100 μs, number of echoes sufficient to complete a decay, 48 logarithmically spaced delay times over the range 10^{-4} – 10^{1} s, and relaxation delay of 10 s. The CPMG acquisition was used to estimate an overall amplitude proportional to the fluid volume (free induction decay [FID] measurement is less informative). Schlumberger editions of 1D and 2D inverse Laplace transform (ILT) techniques were applied while computing the relaxation time distributions [9].

EXPERIMENTAL RESULTS AND DISCUSSION

We choose porous glass with submicron pore sizes (50–300 nm) as the pilot study material, and nanoporous glass (4 and 10 nm) was selected to represent consolidated rock media as the primary study material. All porous samples were studied by a combination of the fluid vapor adsorption/desorption technique and 3D NMR registration.

The experiments began with CPG representing large-scale pore sizes, with capillary condensation effects (an adsorption point when a pore space become filled with a condensed liquid) not expected, and continued with mesoporous silica (pore sizes less than 50 nm). The series of T_2 decays registered at each step of hexane/water vapor adsorption (pressure rise) and desorption (pressure fall) processes was used to construct sorption isotherms. The examples in Figure 2 present the distribution of the relaxation time T_2 obtained by the adsorption of hexane and water vapors in the CPG with pore sizes 300 nm.

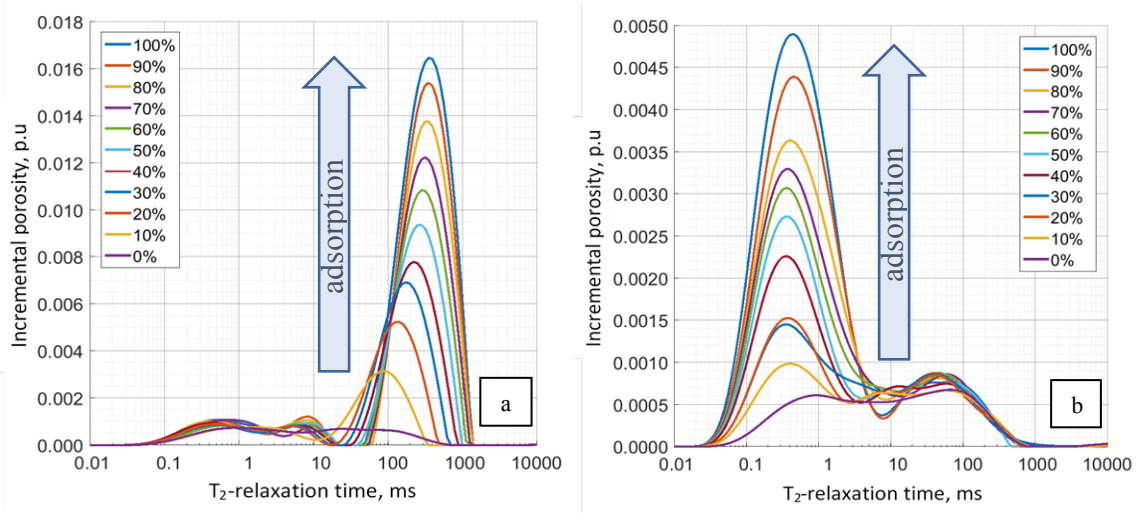

Figure 2. T_2 distributions for adsorption of hexane vapor (a) and water vapor (b) in a CPG sample with 300-nm pore size.

Each T_2 distribution could be averaged with a single value of mean logarithmic T_2 and the sum of the spectra corresponds to the initial amplitude of the T_2 decay curves or to the sorbate volume. The latter was used for plotting adsorption/desorption isotherms (Figure 3), with the logarithmic mean T_2 added to the plots to provide information on confinement states and fluid adhesion. The analysis of logarithmic mean T_2 values instead of calculated full-range T_2 spectra simplifies the interpretation of adsorbed fluid properties at each pressure point.

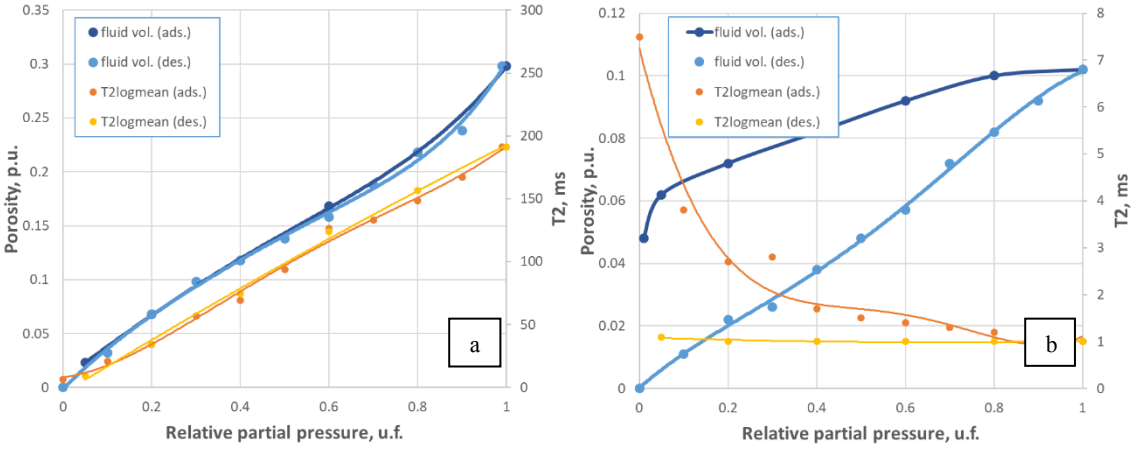

Figure 3. Adsorption/desorption isotherms for hexane (a) and water (b) vapors in a CPG sample with 300-nm pore size and corresponding logarithmic mean T_2 values at each pressure step.

No hysteresis phenomena are observed in the hydrocarbon-related plot (Figure 3a), with the amount of adsorbed fluid (hexane) and its T_2 characteristics increasing monotonically

with increasing of relative pressure and the desorption process showing its reversibility in that the corresponding curve repeats the values obtained for adsorption.
In the second case of the water vapor sorption experiment (Figure 3b), a hysteresis on the adsorption-desorption isotherm is clearly pronounced and the dependence of logarithmic mean times on the relative pressure of the saturated vapor monotonically decreases for the adsorption branch and is almost flat in the desorption process.
For a more detailed study of these features, 2D maps of T_1–T_2 were recorded (Figure 4). The key value for combined interpretation of T_1 and T_2 spectra is their contrast, or T_1/T_2 ratio. Therefore, NMR T_1–T_2 2D maps were analyzed in a slightly rearranged form, in which the y-axis is the T_1/T_2 ratio and the x-axis is T_2.
In the T_1-T_2 graphs (Figure 4), the signal is divided into two areas. In both cases, the peak transverse relaxation time T_2 is about 1 ms, but the peak T_1/T_2 ratio is different: 10 and 1000. The region with a high T_1/T_2 ratio predominates at the initial stages, whereas the low ratio is dominant at higher pressures. Presumably, the region with the high T_1/T_2 corresponds to a first layer of adsorbed fluid molecules, and the region with a low ratio to successive layers. With this interpretation, the fact that during the desorption the area with a high T_1/T_2 ratio does not disappear indicates that the area of the first layer remains unchanged during desorption. This agrees with generally accepted ideas about the desorption process: first, the thickness of the adsorbed layer decreases, and then its surface area decreases.

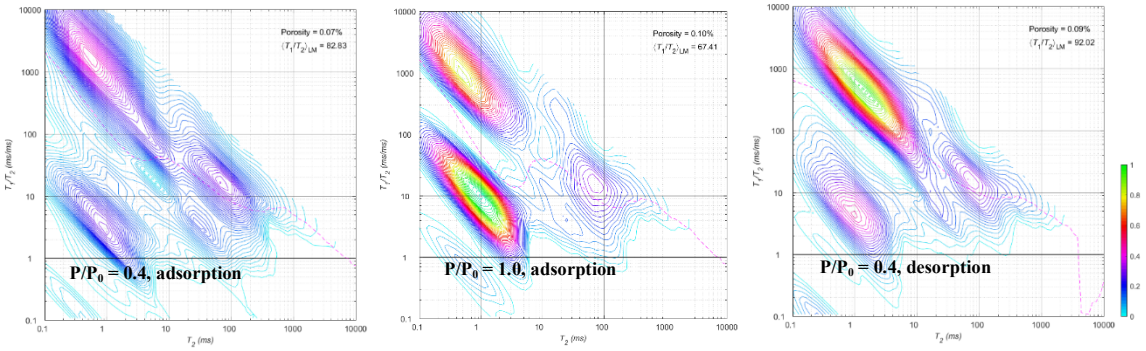

Figure 4. T_1-T_2 maps for selected pressure steps during adsorption/desorption of water vapor in the CPG sample with 300-nm pore size.

Analysis of the NMR data resembles the behavior of the first example (Figures 2a and 3a) for adsorption/desorption processes of hexane vapor in the 50-nm CPG sample. The isotherm branches again duplicate each other and T_2 values monotonically increase with the rise of sorbate volume and decrease as the liquid volume reduces. It is obvious that the processes are fully reversible and are not complicated by surface relaxation phenomena. In other words, the hydrocarbon does not interfere with the solid surfaces, and T_2 changes due to the variation of fluid layer height on the pore surfaces during the adsorption/desorption process. This conclusion is confirmed by the analysis of T_1-T_2 maps for hexane data in that the T_1/T_2 ratios are about unity for all the cases. However, the T_1-T_2 2D maps are not shown in the paper due to page limits, but the form of the distributions is unvaried and corresponds to unimodal 1D distributions of T_2 and T_1.

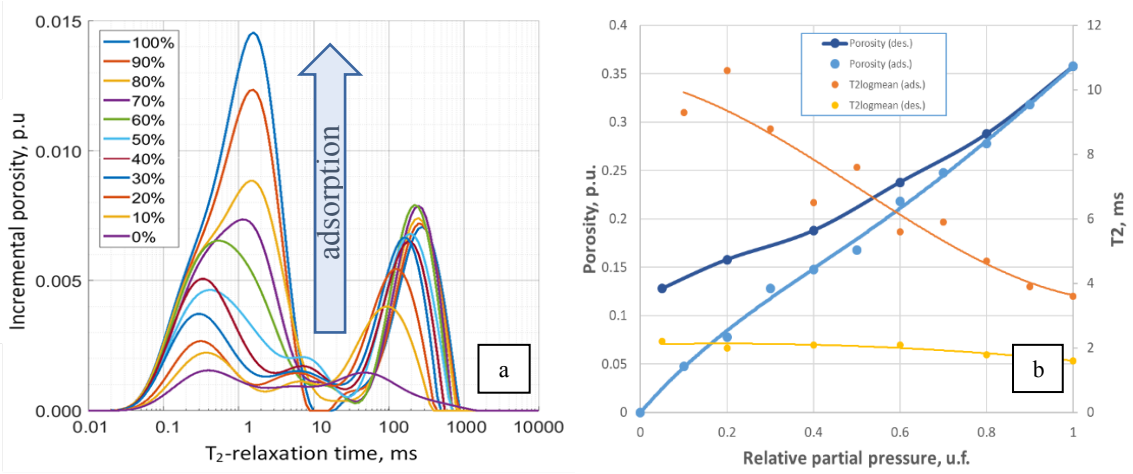

Figure 5. T_2 distributions for adsorption of water vapor (a) and adsorption/desorption isotherms (b) in the CPG sample with 50-nm pore size and corresponding T_2 logarithmic mean values at each pressure step.

Quite different behavior indicates water vapor sorption. A hysteresis loop of the data for the sample with 50-nm pore size shows the desorption curve rises higher in the plot than the adsorption ones (Figure 5b). It is obvious that water requires the application of higher forces to be separated from the pore walls during the desorption process because of its stronger interaction with solid surfaces compared with hexane vapors (water-wet). Contrary to the hexane cases, T_2 values decrease with the rise in sorbate volume, and stay almost constant with the liquid volume reduction (Figure 5b). Analysis of T_2 spectra for the sample with 50-nm pore size confirms this trend (Figure 5a) — modification of water saturation is associated with short-time areas of the distributions (T_2 values less than 10 ms), while long-T_2 modes are almost invariable. This is dictated by a stronger surface relaxivity to water, which indicates a water-wet scenario. Detailed analysis of the T_1-T_2 data confirms the conclusion: the T_1/T_2 ratios are more than an order of magnitude that of hexane. Nevertheless, the 50-nm pore size case is more complicated. This case should be investigated in greater detail than a simple log-mean line or 1D T_2 distribution analysis.

Examples of 2D NMR data for the 50-nm pore size CPG case during water adsorption/desorption processes are presented in Figure 6. As seen in the plots, changes in water saturation during adsorption/desorption processes are reflected at two different areas on the T_1-T_2 maps. The polygon summations were used to quantify the reflection of the T_1-T_2 areas separately. The polygons were drawn manually, and an example of two different polygon calculations is presented in Figure 7. The resulting isotherms for both polygons are presented in different colors (blue: low T_2, red: high T_2) and the arrows show the direction of the adsorption/desorption processes.

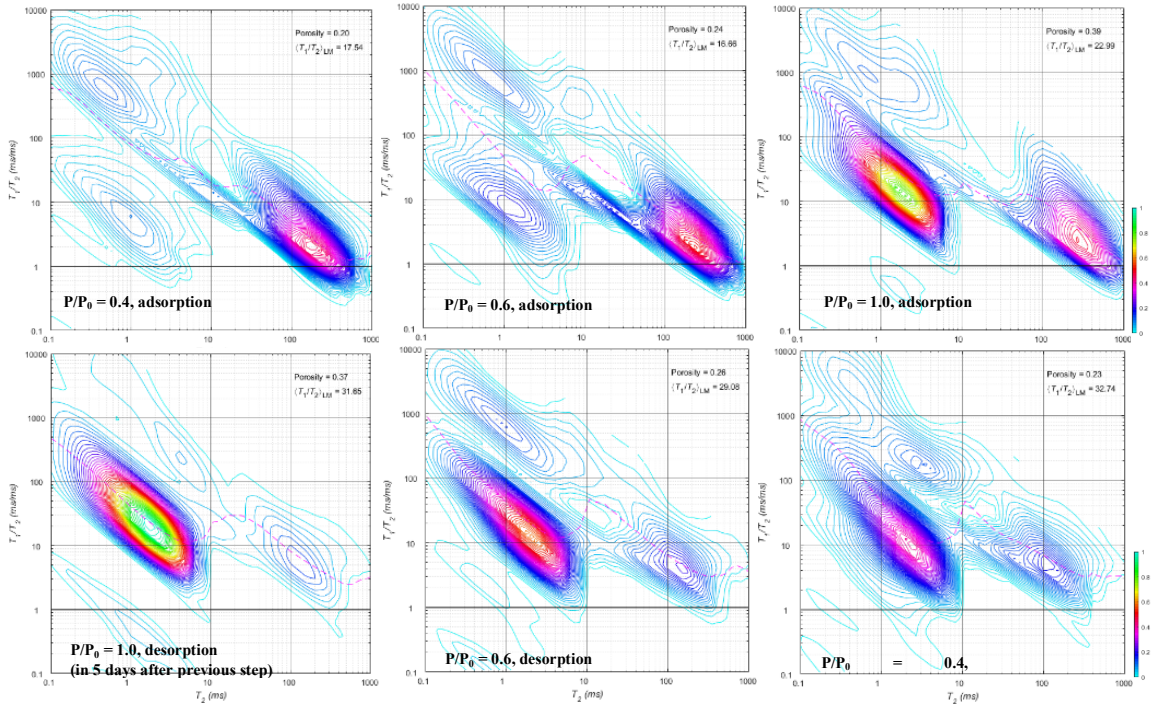

Figure 6. T_1-T_2 maps for selected pressure steps during adsorption/desorption of water vapor in the CPG sample with 50-nm pore size.

The water vapor at the beginning of an adsorption process (up to P/P_0 = 0.4) registers at long T_2 times (100–1000 ms) and lower T_1/T_2 ratios (~4); then the signal is indicated primarily by short T_2 times (0.1–10 ms) and higher T_1/T_2 ratios (~25). The desorption process is the reverse. Such a complex behavior, as well as a narrower hysteresis loop, indicates weaker properties of water wetting and a much slower change in the thickness of the adsorption/desorption water layers due to the smaller pore sizes of the sample along with the formation of large water droplets on the external surface of the sample.

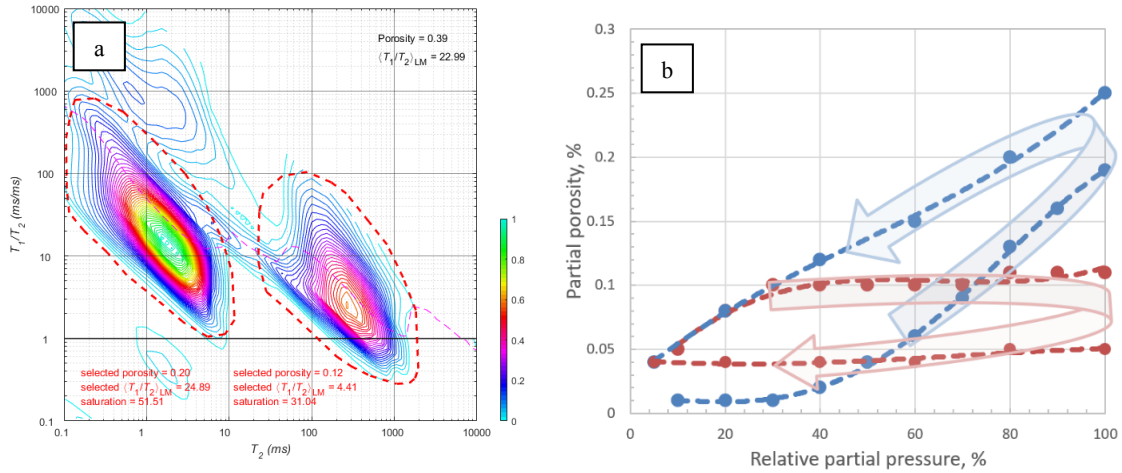

Figure 7. Example of polygon analyses for two areas of T_1-T_2 data for a sample with 50-nm pore size (a) and corresponding adsorption/desorption water vapor isotherms (b).

The final example for 10-nm porous glass is presented in Figure 8 together with routine vapor measurements (ASAP Micromeritics). T_2 analysis shows a monotonic increase with the rise of sorbate volume and decrease with a liquid volume reduction, which is in line with the surface T_2 relaxation phenomena. Much more complicated behavior was observed for T_1-T_2 analysis (Figure 9): T_1 as well as T_2 values monotonically increase up to the beginning of capillary condensation (below $0.6 \cdot P/P_0$), the T_1/T_2 ratio does not change significantly, and then, when capillary condensation occurs, the signal areas are divided into two areas with different T_1/T_2 ratios. The initial low T_1/T_2 area is responsible for monolayer and multimolecular adsorption, while the higher T_1/T_2 area (lower T_2 and higher T_1) corresponds to capillary condensation events within pores and could give its additional characterization. Finally (Figure 9c), most of the fluid is characterized by a similar T_1/T_2 ratio and both T_1 and T_2 distributions reflects the pore morphology: the fluid fills up the pore space and an individual pore is exhibited by a single relaxation rate in terms of the fast-diffusion regime of the NMR acquisition.

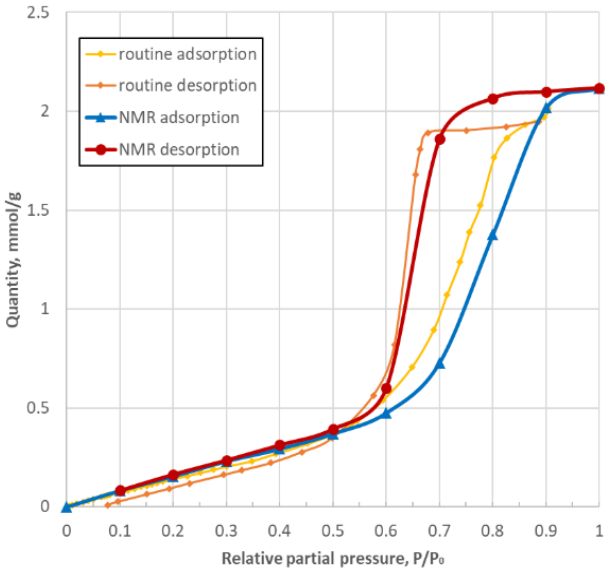

Figure 8. Adsorption-desorption isotherms registered by routine ASAP Micromeritics and NMR-complemented techniques (10-nm porous glass).

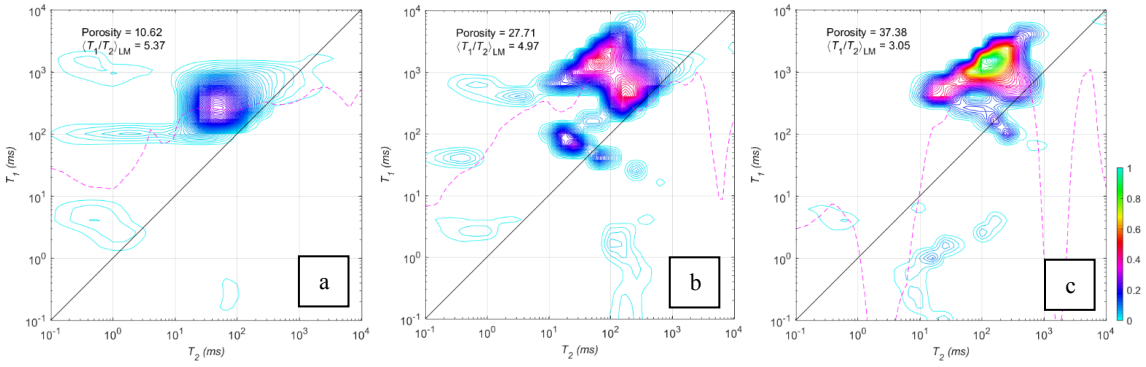

Figure 9. T_1-T_2 data corresponding to 0.3 (a), 0.6 (b), and 0.9 (b) relative pressure points of hexane vapor in 10-nm porous glass.

CONCLUSIONS

The most important achievement of this work is the development of a new complex method for studying both the capacitive and transport-dynamic properties of complex nanoporous materials. The developed NMR-sorption technique gives very similar results compared to an ordinary gas sorption method in terms of registered sorbate volume and significantly enhances it in terms of the characterization of solid-fluid interactions by NMR T_1-T_2 ratios. Registration of NMR characteristics during the recording of adsorption and desorption isotherms of vapors of polar and nonpolar fluids is shown out to be a rich resource of information about the state, properties, and quantity of nanopore fluid adsorbed on the walls. The completed long-lasting series of NMR-sorption experiments with hexane and water vapor and nanopore samples shows not only a capability to quantify hydrogen nuclei volume, but also the robustness of the procedure to characterize sorbate mobility and a degree of fluid-rock interactions during an adsorption/desorption processes. In other words, adsorbed porous fluids can be precisely mapped by their properties and confinement degree.

ACKNOWLEDGEMENTS

I would like to thank Schlumberger for permission to publish this paper. I also acknowledge Dmitry Korobkov and Vera Pletneva for their supports in core preparation and help in conducting core analyses.

REFERENCES

1. Schmidt, R., Stöcker, M., Hansen, E., Akporiaye, D., Ellestad, O.H., "MCM-41: a model system for adsorption studies on mesoporous materials", *Microporous Materials*, 3(4-5), pp. 443-448, 1995.
2. Drago, R.S., Ferris, D.C., Burns, D.S., "Pore-Resolved NMR Porosimetry", *Journal of the American Chemical Society*, 117(26), pp. 6914-6920, 1995.

3. Evenäs, L., Furó, I., Stilbs, P., Valiullin, R., “Adsorption isotherm and aggregate properties of fluorosurfactants on alumina measured by ^{19}F NMR”, *Langmuir*, 18(21), pp. 8096-8101, 2002.
4. Shiko, E., Edler, K.J., Lowe, J.P., Rigby, S.P., “Probing hysteresis during sorption of cyclohexane within mesoporous silica using NMR cryoporometry and relaxometry”, *Journal of Colloid and Interface Science*, 398, pp. 168-175, 2013.
5. Muller, A.C.A., Scrivener, K.L., Gajewicz, A.M., McDonald, P.J., “Use of bench-top NMR to measure the density, composition and desorption isotherm of C-S-H in cement paste”, *Microporous and Mesoporous Materials*, 178, pp. 99-103, 2013.
6. Kwak, H.T., Harbi, A.M., Song, Y., Kleinhammes, A., Wu, Y., “Toward a Method for Measuring Wettability in porous Media by NMR Water Vapor Isotherm Technique”, SCA2017-032.
7. Wua, K., Chena, Z., Lib, J., Lib, X., Xua, J., Donga, X., “Wettability Effect on Nanoconfined Water Flow”, *PNAS*, vol.114, no.13, 3358-3363.
8. Venkataramanan, L., Song, Y.-Q. and Hurlimann, M., "Solving Fredeholm Integrals of the First Kind with Tensor Product Structure in 2 and 2.5 Dimensions", *IEEE Trans. Signal Processing,* vol. 50, pp. 1017-1026, 2002.
9. Mitchell, J., Webber, J.B.W., Strange, J.H., “Nuclear magnetic resonance cryoporometry”, *Physics Reports*, 461(1), pp. 1-36, 2008.